CUPRIAN LIDDICOATITE TOURMALINE

Yusuke Katsurada and Ziyin Sun

Cuprian (copper-bearing) tourmaline, known as "Paraíba" tourmaline in the trade, has been an important gem since its discovery in 1989. Until now, almost all of the material reported has been classified as the elbaite species of the tourmaline supergroup. Chemical analyses by laser ablation–inductively coupled plasma–mass spectroscopy (LA-ICP-MS), a common technique for origin determination of Paraíba tourmalines, revealed that 13 copper-bearing samples submitted to GIA's Tokyo laboratory contained substantial amounts of Ca in the X-site. Consequently, they are classified as liddicoatite tourmaline. The origin of these stones is unknown.

Minerals of the tourmaline supergroup are cyclosilicates with the general formula $XY_3Z_6(T_6O_{18})(BO_3)_3V_3W$, where X = ($Na^+$, Ca^{2+}, K^+, and vacancy); Y = (Fe^{2+}, Mg^{2+}, Mn^{2+}, Cu^{2+}, Al^{3+}, Li^+, Fe^{3+}, and Cr^{3+}); Z = (Al^{3+}, Fe^{3+}, Mg^{2+}, and Cr^{3+}); T = (Si^{4+}, Al^{3+}, and B^{3+}); B = (B^{3+}); V = (OH^- and O^{2-}), and W = (OH^-, F^-, and O^{2-}) (e.g., Henry et al., 2011). Tourmaline-supergroup minerals can be classified into three primary groups based on the X-site occupancy: the alkali group (Na^+ and K^+ dominant), the calcic group (Ca^{2+} dominant), and the X-site vacant group (vacancy dominant). In each primary tourmaline group, specific species are further determined based on the occupancy of other sites. Thirty-four species have been recognized by the International Mineralogical Association's Commission on New Minerals, Nomenclature and Classification (IMA-CNMNC; e.g., Henry et al., 2011; Hawthorne and Dirlam, 2011; B. Dutrow, pers. comm., 2017). Elbaite is a sodium-, lithium-, and aluminum-rich species in the alkali group, with the general formula $(Na)(Li_{1.5}Al_{1.5})Al_6Si_6O_{18}(BO_3)_3(OH)_3(OH)$. Liddicoatite is a calcium- and lithium-rich species in the calcic group, with the general formula $(Ca)(Li_2Al)Al_6Si_6O_{18}(BO_3)_3(OH)_3(OH)$. Most gem-quality tourmaline has been reported as elbaite. Liddicoatite was first distinguished as a separate mineral species in 1977 (Dunn et al., 1977). Gem-quality liddicoatite tourmaline from Madagascar has been prized for its remarkable color zoning that is typically characterized by triangular zones and three-rayed stars surrounded by oscillatory zonings when it is cut perpendicular to the c-axis (e.g., Dirlam et al., 2002; Pezzotta and Laurs, 2011).

Cuprian (copper-bearing) tourmalines with vivid blue, green-blue, green, and violet colors were first reported in 1989 from Paraíba State in northeastern Brazil (Koivula and Kammerling, 1989). They are now commonly called "Paraíba" or "Paraíba-type" tourmaline in the trade. Fritsch et al. (1990) and Bank et al. (1990) reported that the blue to green colors were primarily due to the presence of trace (or minor) amounts of copper. Years after the initial discovery in the state of Paraíba, similar gem-quality elbaite tourmalines colored by copper and manganese were found elsewhere in Brazil (Shigley et al., 2001; Furuya, 2007), in Nigeria (Smith et al., 2001), and in Mozambique (Abduriyim and Kitawaki, 2005; Laurs et al., 2008). The composition of cuprian tourmaline from all of these deposits has been determined with energy-dispersive X-ray fluorescence spectrometry (EDXRF), electron microprobe analysis, and laser ablation–inductively coupled plasma–mass spectroscopy (LA-ICP-MS; see Abduriyim et al., 2006; Okrusch et al., 2016). No mineral species other than elbaite has been previously reported for "Paraíba" tourmalines except for four pieces of Cu-bearing liddicoatite first reported by Karampelas and Klemm (2010) showing Ca-rich X-site occupancy and three

See end of article for About the Authors and Acknowledgments.
GEMS & GEMOLOGY, Vol. 53, No. 1, pp. 34–41,
http://dx.doi.org/10.5741/GEMS.53.1.34

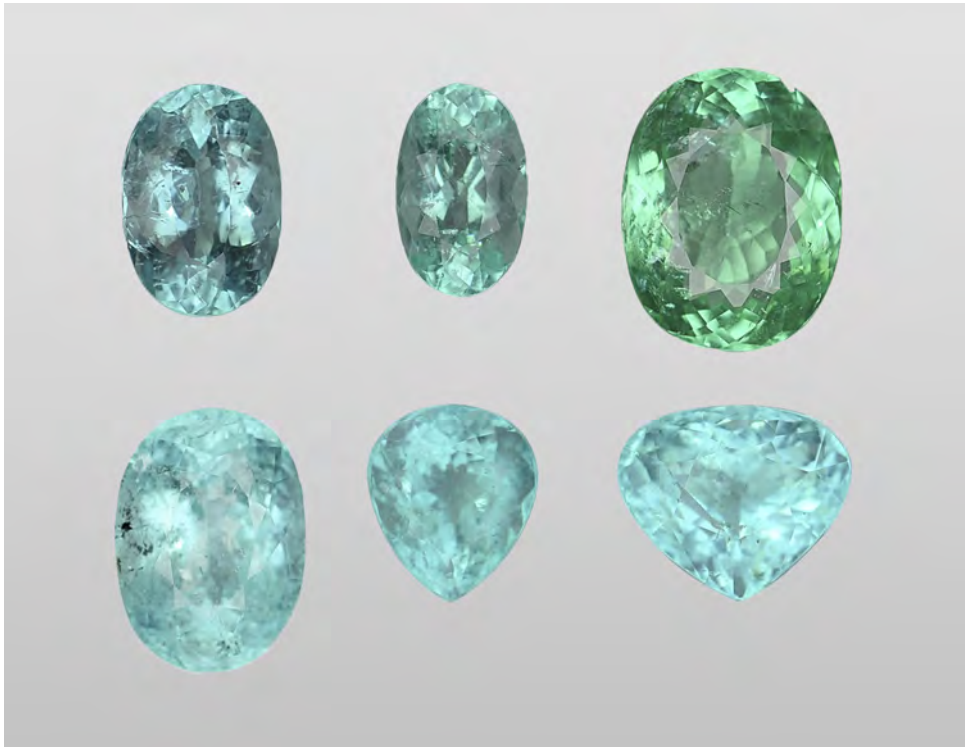

Figure 1. Six of the 13 cuprian liddicoatite tourmalines from this study. The faceted stones weigh 1.59–9.63 ct (average 3.95 ct). They are transparent and have greenish blue, green-blue, and green colors. Photos by Masumi Saito.

pieces of possible liddicoatite conjectured from the qualitative analysis indicating high Ca (Leelawatanasuk and Jakkawanvibul, 2011). This article reports on the same type of cuprian tourmalines that belong to the liddicoatite species based on the evidence supported by quantitative analysis.

MATERIALS AND METHODS

Thirteen tourmaline samples of Paraíba-type colors (figure 1) from unknown geographic origins were examined in GIA's Tokyo laboratory. These were submitted by different clients in 2016. Standard gemological testing was followed by analyses of the major, minor, and trace element concentration for each sample with LA-ICP-MS. Fluorine was not measured. A Thermo Fisher Scientific's iCAP Qc ICP-MS was connected to an Electro Scientific Industries NWR213 laser ablation unit with a frequency-quintupled Nd:YAG laser (213 nm wavelength) running at 4 ns pulse width. NIST SRM 610 and 612 glass standards were used for external calibration. Ablation was achieved using a 40 µm diameter laser spot size, a fluence (energy density) of approximately 10 J/cm^2, and a 7 Hz repetition rate. Three laser spots were acquired from the girdle of each sample. The composition was initially internally standardized with ^{29}Si using a calculated amount of Si based on the weight percent of pure elbaite in the chemical formula. Twenty-six additional cuprian tourmaline samples submitted by clients were analyzed with LA-ICP-MS for comparison. Their geographical origin was identified using GIA's tourmaline database. Eighteen of these additional samples were from Brazil, one from Nigeria, and seven from Mozambique.

The data was converted to wt.% oxides and normalized to 100 wt.% and then converted back to ppmw to obtain individual element concentrations, based on 27 O^{2-} and 4 OH^- anions per formula. LA-ICP-MS analysis for tourmaline is an incomplete characterization, with critical light elements (H and F) and

In Brief

- Almost all copper-bearing tourmaline has been classified as the elbaite species. Cuprian liddicoatite exists, however, and may have entered the "Paraíba" tourmaline market.
- Only sophisticated quantitative chemical analysis can effectively separate liddicoatite from elbaite.
- Cuprian liddicoatite shows high Ga and high Pb. Under long-wave UV, it displays stronger fluorescence than cuprian elbaite due to high concentrations of rare earth elements.

TABLE 1. Chemical composition of 13 cuprian tourmaline samples, obtained by LA-ICP-MS.

Sample no	CT1	CT2	CT3	CT4	CT5	CT6	CT7	CT8	CT9	CT10	CT11	CT12	CT13
							ppmw						
Li	11,600	11,700	12,300	13,600	12,300	12,800	12,500	13,000	13,900	11,700	12,100	12,600	15,300
B	33,900	34,400	33,200	35,200	32,500	34,700	35,200	31,500	33,600	34,400	37,600	34,100	40,300
Na	8920	8480	8050	8390	8960	7600	9130	9860	8170	7910	7120	8220	7810
Al	220000	218,000	230,000	220,000	224,000	217,000	218,000	228,000	225,000	217,000	216,000	222,000	197,000
Si	169,000	169,000	158,000	163,000	166,000	169,000	161,000	164,000	161,000	168,000	164,000	166,000	171,000
Ca	21,000	21,300	24,100	24,400	21,800	21,700	22,800	20,400	23,500	22,200	20,800	22,800	20,400
Mn^{2+}	2160	3110	5780	3610	3480	3340	12,300	2130	3480	6530	8000	2860	10,100
Cu	1490	1610	2120	1510	2140	1600	2790	1550	1460	2300	2510	1330	2970
							atoms per formula unit, 27 O + 4 OH anions normalization						
							X-site						
X site vacancy	0.14	0.15	0.09	0.08	0.11	0.17	0.08	0.11	0.10	0.15	0.22	0.12	0.20
Ca	0.50	0.50	0.57	0.58	0.52	0.51	0.54	0.48	0.56	0.52	0.49	0.54	0.48
Na	0.37	0.35	0.33	0.35	0.37	0.31	0.38	0.41	0.34	0.33	0.29	0.34	0.32
X-site total	1.00	1.00	1.00	1.00	1.00	1.00	1.00	1.00	1.00	1.00	1.00	1.00	1.00
							Y-site						
Al	1.42	1.36	1.46	1.22	1.49	1.30	1.15	1.59	1.37	1.31	1.08	1.37	0.63
Cu	0.02	0.02	0.03	0.02	0.03	0.02	0.04	0.02	0.02	0.03	0.04	0.02	0.04
Li	1.58	1.60	1.70	1.86	1.68	1.74	1.72	1.79	1.90	1.60	1.65	1.73	2.08
Mn^{2+}	0.04	0.05	0.10	0.06	0.06	0.06	0.21	0.04	0.06	0.11	0.14	0.05	0.17
Y-site total	3.06	3.04	3.29	3.16	3.26	3.12	3.13	3.44	3.36	3.06	2.91	3.17	2.92
							Z-site						
Al	6.00	6.00	6.00	6.00	6.00	6.00	6.00	6.00	6.00	6.00	6.00	6.00	6.00
Z-site total	6.00	6.00	6.00	6.00	6.00	6.00	6.00	6.00	6.00	6.00	6.00	6.00	6.00
							T-site						
Si	5.70	5.71	5.35	5.50	5.62	5.68	5.46	5.55	5.46	5.67	5.53	5.58	5.74
Al	0.30	0.29	0.65	0.50	0.38	0.32	0.54	0.45	0.54	0.33	0.47	0.42	0.26
T-site total	6.00	6.00	6.00	6.00	6.00	6.00	6.00	6.00	6.00	6.00	6.00	6.00	6.00
							B-site						
B	2.97	3.01	2.92	3.08	2.85	3.04	3.10	2.77	2.95	3.02	3.29	2.99	3.50
B-site total	2.97	3.01	2.92	3.08	2.85	3.04	3.10	2.77	2.95	3.02	3.29	2.99	3.50
							Sum						
Cation sum	18.89	18.90	19.12	19.17	19.01	18.99	19.15	19.10	19.20	18.93	18.98	19.03	19.22
Anion sum	31.00	31.00	31.00	31.00	31.00	31.00	31.00	31.00	31.00	31.00	31.00	31.00	31.00

Detection limits (ppmw) are: Li (0.95–1.31), B (8.78–10.42), Na (18.91–19.34), Al (3.41–3.48), Ca (339–364), Mn (0.55), and Cu (0.42–0.45). Si is used as internal standard.

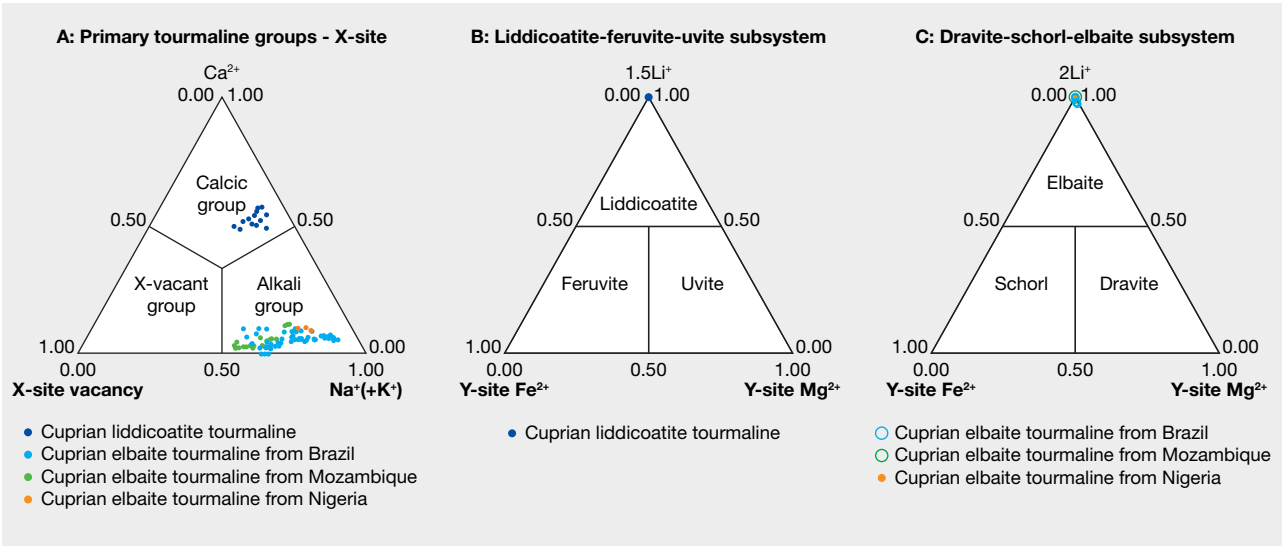

Figure 2. A: The 13 cuprian tourmaline samples belong to the calcic group, while the 26 additional cuprian tourmalines belong to the alkali group based on the dominant occupancy of X-site. B: Li, Y-site Fe^{2+}, and Y-site Mg^{2+} distinguish the tourmaline species as liddicoatite in a liddicoatite-feruvite-uvite subsystem ternary diagram. C: Li, Y-site Fe^{2+}, and Y-site Mg^{2+} of elbaite samples were further plotted in a dravite-schorl-elbaite subsystem ternary diagram (modified after Henry et al., 2011).

the oxidation states of transition elements (Fe and Mn) undetermined. In this article, it is assumed that Fe and Mn are divalent, that the B-site is fully occupied by B, and that the X-site is occupied by Na, Ca, and a vacancy equal to 1 atom per formula unit (apfu). Additional assumptions are that the Z-site is only occupied by Al^{3+} and equal to 6 apfu, while the T-site is occupied by Si^{4+} and Al^{3+} and equal to 6 apfu. If Si^{4+} is greater than 6, the T-site is only occupied by Si^{4+}. The excess Al goes into the Y-site. The priority of ions with different valence states entering the Y-site is ($R^{2+} > R^{3+} > R^{+} > R^{4+}$), such that the Y-site is occupied by Mn, Cu, Al, and Li. The common assumption that all iron is ferrous and that OH + F = 4 apfu can result in the misidentification of buergerite as "fluor-schorl" as well as misidentification of the oxy- and fluor- species. The chemical composition presented in this article is not affected by the minor amounts of Fe in the tourmaline (Clark, 2007). The assumption of 4 OH^- does not allow for the fluor- or oxy- species to be determined. The major elements, including Ca, Na, Si, Al, and Mg, were verified by comparison of LA-ICP-MS data with electron microprobe data of a secondary tourmaline standard with similar Ca:Na ratios (Dutrow and Henry, pers. comm., 2017).

RESULTS AND DISCUSSIONS

Microscopic examination of the 13 samples revealed two-phase inclusions, needle-like growth tubes, and fluid inclusions typical of tourmaline. Standard gemological testing resulted in the general range of gem tourmalines such as refractive indices of 1.62–1.64 and specific gravity of approximately 3.06, but the fluorescence under long-wave ultraviolet light was stronger than the usual Paraíba tourmalines, as described later. Chemical analysis demonstrated a calcium-dominant composition. The representative data in table 1 was selected to show the best stoichiometry. All the data points showed liddicoatite, and none were classified as elbaite. In all analyses, Mg was below the detection limit and Fe was less than 0.005 apfu. Based on the primary tourmaline group classification, all 13 calcium-rich cuprian samples are classified as calcic-group tourmaline and the 26 additional sodium-rich cuprian samples as alkali-group tourmaline (table 2, figure 2A). In addition, the 13 calcic-group samples plot as liddicoatite tourmaline in a liddicoatite-feruvite-uvite subsystem ternary diagram (figure 2B). The 26 tourmalines in the alkali group are shown as elbaite in a dravite-schorl-elbaite subsystem ternary diagram (figure 2C; Henry et al., 2011).

Comparing the data in table 1 with that of liddicoatitic tourmaline from Madagascar (Dirlam et al., 2002) shows that these cuprian samples have more sodium in the X-site—with a greater elbaitic component. Other liddicoatite tourmalines from Canada (Teertstra et al., 1999) have similar sodium (0.365–

TABLE 2. X-site occupancy of 26 cuprian elbaite samples in molecular proportions, obtained by LA-ICP-MS.

	Na	K	Ca	Vacancy
Brazil	0.705 (0.513–0.861)	0.003 (0.001–0.005)	0.063 (0.000–0.112)	0.229 (0.073–0.381)
Mozambique	0.596 (0.519–0.661)	0.002 (0.002–0.003)	0.057 (0.025–0.131)	0.346 (0.205–0.444)
Nigeria	0.724 (0.699–0.748)	0.003 (0.003–0.003)	0.111 (0.103–0.116)	0.162 (0.145–0.185)

0.395 apfu) and similar or lower calcium (0.420–0.498 apfu). The sodium contents of liddicoatite from Madagascar and Canada vary with their zonation.

Table 3 shows the samples' averaged chemical composition for selected minor and trace elements. In cuprian tourmalines from different origins, these have some distinguishable trends (Abduriyim et al., 2006; Okrusch et al., 2016). For example, Brazilian and Nigerian cuprian tourmalines tend to show higher concentrations of Cu than those from Mozambique—which typically have higher Ga than the other two sources. Nigerian stones tend to have higher Pb than those from Brazil and Mozambique. Figure 3 shows the Ga-Pb distribution of the 13 cuprian liddicoatite and 26 cuprian elbaite samples analyzed in this study. The cuprian liddicoatite samples show both high Ga (297–433 ppmw) and high Pb (420–827 ppmw). These combinations of trace elements plot well outside the ranges of any known reference samples in GIA's database, and therefore their geographic origin could not be determined.

Another remarkable point was the samples' high concentration of rare earth elements (REE; table 2)—in other words, lanthanides except Pm. Lighter REE (La, Ce, Pr, Nd, Sm, and Gd) showed a higher concentration than heavier REE (Tb, Dy, Ho, Er, Tm, Yb, and Lu). The samples show an exceptionally low Eu content. The high concentration of REEs is interpreted as the cause of their comparatively strong fluorescence under long-wave UV (figure 4).

Although the geographic origin of these cuprian liddicoatite is unknown, this unique chemical property offers directions for further research. Geological studies of the elbaitic cuprian tourmaline deposits in Brazil have been published (e.g., Shigley et al., 2001; Soares et al., 2008; Beurlen et al., 2011), but no detailed study has been carried out for Nigerian and Mozambican occurrences. Teertstra et al. (1999) reported that some liddicoatite crystals have cores that correspond to elbaite with rims of liddicoatite. They proposed three possibilities for the calcium needed to form liddicoatite: mobilization of Ca from earlier-formed pegmatite minerals, introduction of Ca from host rocks, and conservation of Ca through the crystallization of minerals in the pegmatite magma. Major elements can also be used to determine provenance. Henry and Guidotti (1985) established distinct regions to define potential different source rock types of tourmaline using Al-Fe(tot)-Mg and Ca-Fe(tot)-Mg ternary diagrams. Figure 5 indicates that the rock

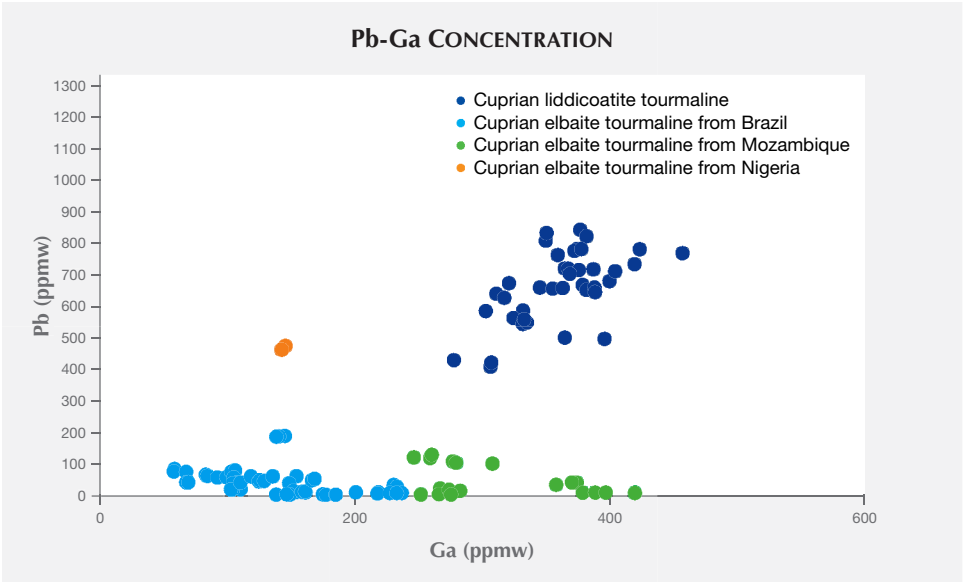

Figure 3. Pb vs. Ga concentration plot of the 13 cuprian liddicoatites of unknown origin and 26 cuprian elbaite tourmalines from Brazil, Mozambique, and Nigeria. The 13 cuprian liddicoatites have high Pb and high Ga. Cuprian elbaite tourmalines from Brazil have low Pb and low Ga. Cuprian elbaites from Mozambique have high Ga and low Pb, while those from Nigeria have low Ga and high Pb.

TABLE 3. Minor and trace element concentration (ppmw) of 13 cuprian liddicoatite samples and 26 cuprian elbaites from Brazil, Mozambique, and Nigeria.

Sample	CT1	CT2	CT3	CT4	CT5	CT6	CT7	CT8	CT9	CT10	CT11	CT12	CT13	Brazil (18 samples)	Mozambique (7 samples)	Nigeria (1 sample)
Mg	bdl	1.90	bdl	bdl	bdl	bdl	bdl	bdl	bdl	bdl	bdl	bdl	0.25	112 (0–1170)	bdl	0.73
Mn^{2+}	2220	3140	5740	3570	3510	3440	12300	2130	3430	6490	7900	2790	9820	11800 (420–26300)	4360 (99.5–12100)	18700
Fe^{2+}	bdl	261	72.4	66.0	34.9	20.0	208	bdl	36.0	155	241	42.9	201	164 (0–1060)	bdl	209
Cu	1530	1580	2100	1490	2140	1650	2850	1560	1530	2250	2550	1220	2860	9580 (420–23200)	2310 (1140–3430)	2470
Ga	397	373	333	368	382	375	297	433	359	324	319	376	349	139 (61.2–232)	321 (255–401)	143
La	4.99	17.0	76.9	42.6	27.9	42.2	108	4.28	42.8	87.3	99.9	27.5	93.2	0.69 (bdl–3.72)	0.01 (bdl–0.03)	0.04
Ce	20.3	54.2	230	131	88.1	131	316	20.0	137	277	304	92.0	319	0.97 (bdl–5.79)	0.02 (bdl–0.06)	0.04
Pr	4.89	9.62	31.2	18.9	15.5	19.6	40.5	5.06	19.8	32.6	39.9	11.8	39.5	0.07 (bdl–0.42)	0.00 (bdl–0.00)	0
Nd	36.5	47.1	111	76	72.2	71.9	126	37.3	72.4	115	123	65.0	120	0.12 (bdl–0.82)	bdl	bdl
Sm	40.0	29.5	27.0	26.7	58.3	26.6	26.0	45.7	27.8	25.6	28.8	23.0	28.0	0.02 (bdl–0.13)	bdl	bdl
Eu	1.26	0.79	0.63	0.64	1.57	0.75	0.64	1.64	0.73	0.77	0.71	0.69	0.71	0.00 (bdl–0.01)	bdl	bdl
Gd	12.2	8.25	7.65	6.84	15.1	6.43	7.59	13.3	7.48	7.15	8.22	6.44	6.71	0.01 (bdl–0.06)	0.00 (bdl–0.02)	bdl
Tb	0.89	0.51	0.43	0.40	1.18	0.41	0.48	0.86	0.39	0.45	0.51	0.34	0.46	0.00 (bdl–0.01)	bdl	0
Dy	1.48	1.00	0.82	0.66	1.67	0.79	0.79	1.44	0.71	0.77	0.92	0.84	0.75	0.00 (bdl–0.01)	bdl	bdl
Ho	0.08	0.06	0.04	0.04	0.07	0.05	0.05	0.10	0.05	0.05	0.06	0.03	0.06	0.00 (bdl–0.00)	0.00 (bdl–0.00)	bdl
Er	0.09	0.09	0.10	0.06	0.10	0.13	0.09	0.07	0.10	0.09	0.09	0.07	0.08	0.00 (bdl–0.00)	0.00 (bdl–0.01)	bdl
Tm	bdl	0.00	0.01	0.01	0.00	0.01	0.00	0.01	bdl	0.00	bdl	0.00	0.01	0.00 (bdl–0.01)	0.00 (bdl–0.00)	bdl
Yb	0.08	0.05	0.02	bdl	0.05	0.04	bdl	0.07	0.03	0.01	bdl	0.05	bdl	0.00 (bdl–0.01)	0.00 (bdl–0.01)	bdl
Lu	0.01	bdl	0.01	0.00	bdl	bdl	0.01	0.01	bdl	bdl	bdl	0.00	bdl	0.02 (bdl–0.40)	bdl	bdl
Ta	7.31	6.52	5.30	7.18	5.06	6.85	4.18	8.05	7.92	6.53	6.70	7.70	5.83	2.23 (0.04–8.35)	1.58 (0.54–3.62)	6.66
Pb	703	672	550	773	659	774	420	761	827	642	578	567	684	44.4 (2.74–188)	43.9 (3.85–123)	467
∑REE	123	168	486	304	282	300	626	130	309	547	606	228	609	1.89	0.03	0.1

Abbreviation: bdl = below detection limit. Detection limits (ppmw) are: Mg (0.13–0.56), Mn (0.16–1.01), Fe (6.70–34.02), Cu (0.73–3.00), Ga (0.05–0.19), La (0.00–1.26), Ce (0.00–0.01), Pr (0.00–0.02), Nd (0.00–0.23), Sm (0.00–0.04), Eu (0.00–0.01), Gd (0.00–0.02), Tb (0.00–0.01), Dy (0.00–0.02), Ho (0.00), Er (0.00–0.01). Tm (0.00–0.01), Yb (0.01–0.02), Lu (0.00–0.01), Ta (0.00), and Pb (0.05–0.14).

types in which the cuprian liddicoatite was found are Li-rich granitoid pegmatites and aplites. Because these copper-bearing liddicoatite tourmalines are Ca-dominant, they must be from a Ca-rich host rock. Karampelas and Klemm (2010) noted that liddicoatite rough had been found near the Paraíba-type el-

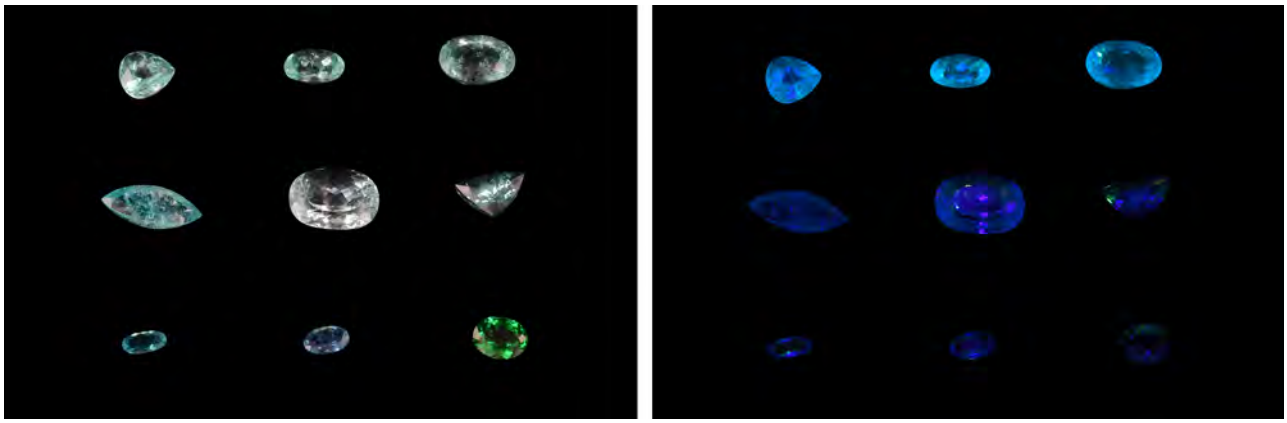

Figure 4. Randomly selected samples under daylight-equivalent light (left) and under long-wave UV light (right). Copper-bearing liddicoatite (CT05, CT03, and CT06 at the top) show stronger fluorescence than the cuprian elbaite (MZ04, MZ06, NG01, BR15, BR17, and BR08 at the middle and bottom) due to high REE concentrations. Photos by Yusuke Katsurada.

baite mine in Mozambique. Qualitative EDXRF analysis of Paraíba-type tourmaline from a new mine reportedly near Nampula, Mozambique, showed a Ca peak (Leelawatanasuk and Jakkawanvibul, 2011).

Figure 5. A: This Al-Fe(tot)-Mg diagram (in molecular proportions) reveals that the likely source rock of cuprian liddicoatite tourmaline is Li-rich granitoid pegmatite and aplite. Fe(tot) represents the total Fe. This diagram is divided into regions that define the compositional range of tourmaline from different rock types (modified after Henry and Guidotti, 1985). B: The Ca-Fe(tot)-Mg diagram (also in molecular proportions) shows that the likely source rock of cuprian liddicoatite tourmaline is Li-rich granitoid pegmatite and aplite. The rock types defined by the fields in this diagram (also modified after Henry and Guidotti, 1985) are somewhat different from those in figure 5A.

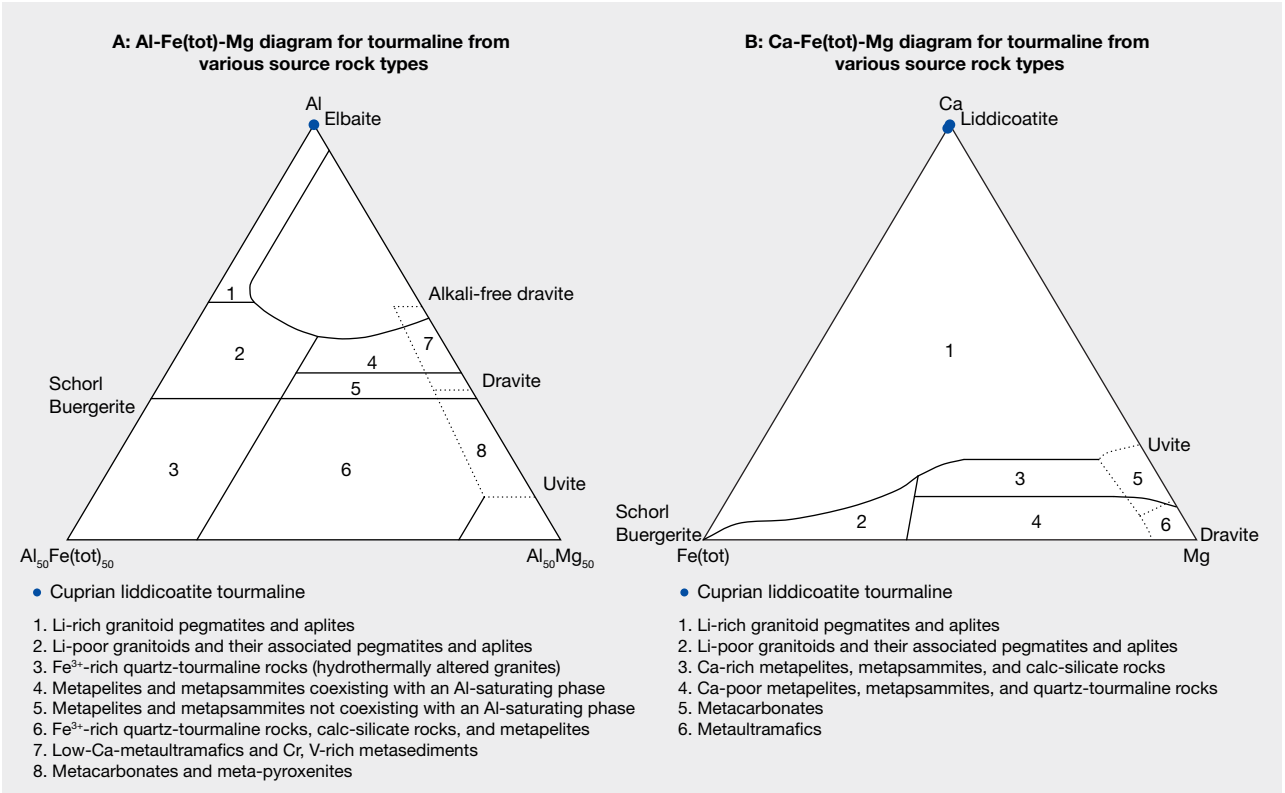

Analysis of the host rock geology around cuprian tourmaline mines in Mozambique may be an important approach.

CONCLUSIONS

Thirteen cuprian tourmaline samples were identified as liddicoatite tourmaline. Their Cu and Mn concentrations were within the range of other cuprian tourmalines—consistent with their similar blue to green colors. Except for their stronger fluorescence under long-wave UV, presumably caused by high REE concentrations, the samples' gemological properties were also similar to cuprian elbaite tourmalines. Only sophisticated quantitative chemical analyses can effectively separate liddicoatite from elbaite.

Cuprian liddicoatite tourmaline is not well known, but the material may have already entered the "Paraíba" tourmaline market. Discovering its origin could provide new insights into the geologic growth conditions and chemical variations of tourmaline crystals.

ABOUT THE AUTHORS

Dr. Katsurada is a scientist and a staff gemologist at GIA in Tokyo. Mr. Sun is a staff gemologist at GIA in Carlsbad, California.

ACKNOWLEDGMENTS

We wish to thank Dr. Makoto Miura and Takuya Sunaoshi of GIA's laboratory in Tokyo for assisting with LA-ICP-MS testing. We also appreciate the helpful comments and suggestions from Shane McClure of GIA Carlsbad and Dr. Barbara Dutrow of Louisiana State University.

REFERENCES

Abduriyim A., Kitawaki H. (2005) Gem News International: Cu- and Mn-bearing tourmaline—More production from Mozambique. *G&G*, Vol. 41, No. 4, pp. 360–361.

Abduriyim A., Kitawaki H., Furuya M., Schwarz D. (2006) "Paraíba"-type copper-bearing tourmaline from Brazil, Nigeria, and Mozambique: Chemical fingerprinting by LA-ICP-MS. *G&G*, Vol. 42, No. 1, pp. 4–21, http://dx.doi.org/10.5741/GEMS.42.1.4

Bank H., Henn U., Bank F.H., von Platen H., Hofmeister W. (1990) Leuchtendblaue Cu-führende Turmaline aus Paraiba, Brasilien. *Zeitschrift der Deutschen Gemmologischen Gesellschaft*, Vol. 39, No. 1, pp. 3–11 (in German).

Beurlen H., de Moura O. J.M., Soares D. R., Da Silva M. R.R., Rhede D. (2011) Geochemical and geological controls on the genesis of gem-quality "Paraíba tourmaline" in granitic pegmatites from northeastern Brazil. *The Canadian Mineralogist*, Vol. 49, No. 1, pp. 277–300, http://dx.doi.org/10.3749/canmin.49.1.277

Clark C.M. (2007) Tourmaline: Structure formula calculations. *The Canadian Mineralogist*, Vol. 45, No. 2, pp. 229–237, http://dx.doi.org/10.2113/gscanmin.45.2.229

Dirlam D.M., Laurs B.M., Pezzotta F., Simmons W.B. (2002) Liddicoatite tourmaline from Anjanabonoina, Madagascar. *G&G*, Vol. 38, No. 1, pp. 28–53, http://dx.doi.org/10.5741/GEMS.38.1.28

Dunn P.J., Appleman D.E., Nelen J.E. (1977) Liddicoatite, a new calcium end-member of the tourmaline group. *American Mineralogist*, Vol. 62, pp. 1121–1124.

Fritsch E., Shigley J.E., Rossman G.R., Mercer M.E., Muhlmeister S.M., Moon M. (1990) Gem-quality cuprian-elbaite tourmalines from São José da Batalha, Paraíba, Brazil. *G&G*, Vol. 26, No. 3, pp. 189–205, http://dx.doi.org/10.5741/GEMS.26.3.189

Furuya M. (2007) Copper-bearing tourmaline from new deposits in Paraíba State, Brazil. *G&G*, Vol. 43, No. 3, pp. 236–239, http://dx.doi.org/10.5741/GEMS.43.3.236

Hawthorne F.C., Dirlam D.M. (2011) Tourmaline the indicator mineral: From atomic arrangement to Viking navigation. *Elements*, Vol. 7, No. 5, pp. 307–312, http://dx.doi.org/10.2113/gselements.7.5.307

Henry D.J., Guidotti C.V. (1985) Tourmaline as a petrogenetic indicator mineral: an example from the staurolite-grade metapelites of NW Maine. *American Mineralogist*, Vol. 70, pp. 1–15.

Henry D.J., Novák M., Hawthorne F.C., Ertl A., Dutrow B.L., Uher P., Pezzotta F. (2011) Nomenclature of the tourmaline-supergroup minerals. *American Mineralogist*, Vol. 96, No. 5–6, pp. 895–913, http://dx.doi.org/10.2138/am.2011.3636

Karampelas S., Klemm L. (2010) Gem News International: "Neon" blue-to-green Cu- and Mn-bearing liddicoatite tourmaline. *G&G*, Vol. 46, No. 4, pp. 323–325.

Koivula J.I., Kammerling R.C., Eds. (1989) Gem News: Paraíba tourmaline update. *G&G*, Vol. 25, No. 4, pp. 248–249.

Laurs B.M., Zwaan J.C., Breeding C.M., Simmons W.B., Beaton D., Rijsdijk K.F., Befi R., Falster A.U. (2008) Copper-bearing (Paraíba-type) tourmaline from Mozambique. *G&G*, Vol. 44, No. 1, pp. 4–30, http://dx.doi.org/10.5741/GEMS.44.1.4

Leelawatanasuk T., Jakkawanvibul J. (2011) New Paraiba-type tourmaline from Mozambique. http://www.git.or.th/2014/eng/testing_center_en/lab_notes_en/glab_en/2011/GIT_Paraiba-new_Mine.pdf.

Okrusch M., Ertl, A., Schüssler U., Tillmanns E., Brätz H., Bank H. (2016) Major- and trace-element composition of Paraíba-type tourmaline from Brazil, Mozambique and Nigeria. *The Journal of Gemmology*, Vol. 35, No. 2, pp. 120–139.

Pezzotta F., Laurs B.M. (2011) Tourmaline: the kaleidoscopic gemstone. *Elements*, Vol. 7, No. 5, pp. 333–338, http://dx.doi.org/10.2113/gselements.7.5.333

Shigley J.E., Cook B.C., Laurs B.M., Oliveira Bernardes M. (2001) An update on "Paraíba" tourmaline from Brazil. *G&G*, Vol. 37, No. 3, pp. 260–276, http://dx.doi.org/10.5741/GEMS.37.4.260

Smith C.P., Bosshart G., Schwartz D. (2001) Gem News International: Nigeria as a new source of copper-manganese-bearing tourmaline. *G&G*, Vol. 37, No. 3, pp. 239–240.

Soares D.R., Beurlen H., Barreto S. d. B., Da Silva M.R.R., Ferreira A.C.M. (2008) Compositional variation of tourmaline-group minerals in the Borborema pegmatite province, northeastern Brazil. *The Canadian Mineralogist*, Vol. 46, No. 5, 1097–1116, http://dx.doi.org/10.3749/canmin.46.5.1097

Teertstra D.K., Černý P., Ottolini L. (1999) Stranger in paradise: Liddicoatite from the High Grade Dike pegmatite, southeastern Manitoba, Canada. *European Journal of Mineralogy*, Vol. 11, No. 2, pp. 227–235, http://dx.doi.org/10.1127/ejm/11/2/0227